

Analysis of extreme weather hazards in Aceh Besar Regency, Indonesia, using a geospatial approach

Ahmad Farhan^{1,2}, Muhammad Syukri^{1,3*}, Saumi Syahreza^{1,3}, Taufan Hidayat^{1,4}

¹ Graduate School of Mathematics and Applied Science, Universitas Syiah Kuala, Banda Aceh, 23111, Indonesia

² Department of Physics Education, Faculty of Teacher Training and Education, Universitas Syiah Kuala, Darussalam, Banda Aceh 23111, Indonesia

³ Department of Physics, Faculty of Mathematics and Natural Sciences, Universitas Syiah Kuala, Banda Aceh, 23111, Indonesia

⁴ Department of Agrotechnology Faculty of Agriculture, Universitas Syiah Kuala, Darussalam, Banda Aceh 23111, Indonesia

* Corresponding author's e-mail: m.syukri@usk.ac.id

ABSTRACT

Aceh Besar Regency, Indonesia, as a tropical region, frequently experiences extreme weather events, including strong winds that can have significant impacts. This study aims to analyze extreme weather hazards using a geospatial approach by applying overlay techniques within a Geographic Information System (GIS). The methodology involves mapping slope scores, classifying land cover, assessing rainfall patterns, and generalizing slope classes to generate an extreme weather hazard map. The results indicate that the average area of low-hazard zones per village is 0.198 km², with a standard deviation of 1.057 km², while moderate-hazard zones have an average area of 3.90 km² with a standard deviation of 13.59 km². Notably, the majority of villages (88.2%) do not contain significant low-hazard areas (0 km²), whereas moderate-hazard zones are more widely distributed across villages. Further analysis reveals that villages classified as high-hazard areas are predominantly located at higher elevations or within transitional zones between lowlands and highlands. The spatial distribution of hazard levels correlates with topographic conditions, proximity to rivers, and land-use patterns. These findings provide valuable insights for local governments in developing data-driven disaster mitigation strategies to reduce the risks associated with extreme weather events.

Keywords: spatial assessment, extreme weather hazard, Aceh Besar, mitigation, planning.

INTRODUCTION

Aceh Besar Regency, Indonesia, located in a tropical region, experiences two primary seasons: the rainy season and the dry season. The transition between these seasons is often accompanied by extreme weather events, one of the most notable being strong winds. In tropical regions, strong winds commonly occur during the transition from the dry to the rainy season, influenced by the movement of monsoonal winds originating from Australia. Generally, these winds are more frequent in mountainous or highland areas, as well as regions with minimal vegetation cover. Several factors contribute to the occurrence of strong

winds, including atmospheric pressure variations within weather systems, increases in air pressure, and the apparent movement of the sun at its zenith (solar culmination). The impact of strong winds can lead to significant physical and economic losses, necessitating effective mitigation measures to reduce associated risks. In disaster mitigation efforts, Indonesia has implemented Law No. 24 of 2007 on Disaster Management, which emphasizes a paradigm shift from reactive response strategies toward proactive risk reduction approaches (BNPB, 2012). As key stakeholders, local governments are responsible for conducting systematic and data-driven disaster risk assessments. These assessments aim to identify and

understand the characteristics of existing hazards while developing effective adaptation strategies to minimize long-term impacts on communities and their assets. A comprehensive disaster risk assessment serves as the foundation for regional disaster management planning. It informs the development of various policy documents, including disaster management plans, risk reduction strategies, contingency plans, and post-disaster recovery frameworks.

To ensure the reliability and scientific validity of disaster risk assessments, methodologies must be based on accurate and verifiable data. As part of Indonesia national priorities, disaster management has become a fundamental agenda for local governments. Within this context, there is an increasing need for expertise in risk assessment methodologies and techniques, particularly concerning extreme weather events. One such extreme weather phenomenon of concern is strong winds, defined as winds reaching speeds of ≥ 120 km/h. In tropical regions, especially between the Tropic of Cancer and the Tropic of Capricorn, strong winds frequently occur due to atmospheric pressure differentials, increases in air pressure, and the apparent movement of the sun, which influences solar culmination (Wang et al., 2006).

Several researchers have highlighted the use of a geospatial approach for hazard assessment by applying overlay techniques within the GIS. A self-organizing map, a type of artificial neural network, was used to analyze three decades of rainfall data in Nigeria, identifying four distinct precipitation zones and revealing an increasing trend in rainy days in the northern region (Akande et al., 2017). Sentinel-2A data and the Vegetation Condition Index were used to monitor agricultural drought in Aceh Besar, revealing a mild drought trend and increasing vulnerability in paddy rice fields from 2018 to 2022 (Sugianto et al., 2023). A GIS-MCA framework incorporating the analytical hierarchy process (AHP), the technique for order preference by similarity to the ideal solution (TOPSIS), and ordered weighted averaging (OWA) was applied to map flood hazard zones in the Dadu River basin, China, identifying high-risk areas and validating the approach as effective for flood management (Chen, 2022). A GIS-based study assessed flash flood vulnerability in the Valea Rea catchment, Romania, revealing that 43% of the area is highly susceptible, posing risks to communities and

infrastructure (Kocsis et al., 2022). A GIS and RS-based flood hazard assessment in the Gidabo Watershed identified 41.6% of the area as highly susceptible, with the risk map validated at 0.943 ROC accuracy (Diriba, et al., 2024). A GIS and MCDA-based study, including IR'AHP, mapped urban flood hazard zones in Palilula, Belgrade, identifying high-risk areas along the Danube and validating results with historical flood data (Gigović et al., 2017). GIS and IDW interpolation were used to assess extreme flood impacts on agriculture in Quang Nam, Vietnam, revealing that up to 33% of arable land, particularly wet rice fields, is inundated under severe flood scenarios (Chau et al., 2013). Landslide hazard zonation was evaluated in Meta Robi District, Ethiopia, using Grid Overlay and GIS modeling, demonstrating that GIS modeling is highly accurate and efficient, with 95% of past landslides occurring in high-hazard zones (Raghuvanshi, 2015). A GIS-based approach utilizing remote sensing and AHP was applied to create a landslide susceptibility map for Balakot, Pakistan, identifying high-risk zones with 76% accuracy for hazard mitigation and land use planning (Basharat, et al., 2016). The use of remote sensing data for landslide detection, monitoring, and hazard prediction in Switzerland was explored, leading to the development of a GIS-based expert tool under HazNETH to enhance natural hazard assessment (Metternicht et al., 2005).

A GIS-based multi-criteria framework integrating geospatial data, AHP, and a Social Vulnerability Index assessed multi-hazard risk in Dharan, Nepal, identifying high-risk zones along the Seuti and Sardu Rivers for disaster planning (Aksha et al., 2020). A Coastal Vulnerability Index was developed using spatial analysis to assess multi-hazard risks along Bangladesh's eastern coast, revealing that 32% of the coastline is highly vulnerable, with results validated through field observations (Hoque et al., 2020). A spatial multi-criteria approach using remote sensing and AHP was developed to map tropical cyclone risk in coastal Bangladesh, identifying high-risk areas and validating its effectiveness for disaster planning (Hoque et al., 2018). A GIS-based integrated approach for bushfire risk assessment was developed, combining spatial data integration, hazard simulation, and multi-criteria evaluation to support effective risk decision-making (Chen et al., 2003). A GIS-based Boolean overlay and weighted linear combination (WLC)

method was used to identify suitable rainwater harvesting sites in Iraq’s western desert, revealing that only 6% of the area is highly suitable for rainwater harvesting, supporting efficient water management in arid regions (Hashim and Sayl, 2021). Soil suitability for cotton cultivation in the Ringanbodi watershed, India, was evaluated using GIS-based multi-criteria analysis, revealing that 49.1% of the area is moderately suitable, while 16.6% is unsuitable due to soil limitations (Walke et al., 2012). A GIS-based study assessed earthquake disaster risk in Bener Meriah, Indonesia, revealing that the 2013 earthquake caused significant physical and economic losses, with risk levels categorized as medium and low (Farhan et al., 2024). Remote sensing techniques were employed to estimate land surface temperature in the Mount Seulawah geothermal area, identifying temperature anomalies and high lineament density, indicating strong geothermal potential for sustainable development (Akhyar and Sary, 2024). Planetscope-3A imagery and supervised classification were used to map green open spaces (GOS) in Banda Aceh, revealing that 35.29% of the area consists of GOS, with an overall accuracy of 76.04% (Budi and Akhyar, 2021).

This study aims to analyze extreme weather hazards in Aceh Besar Regency, Indonesia, to support mitigation planning using geospatial analysis with overlay techniques in a GIS. The hazard mapping process follows the standards established by the Indonesian National Disaster Management Agency (BNPB) and consists of several analytical stages: (1) generating a slope score map, (2) classifying and scoring land cover, (3) developing a rainfall score map, and (4) creating a generalized slope class map. These datasets are then integrated to produce an extreme weather hazard map for Aceh Besar Regency. The findings of this study are expected to contribute to the development of data-driven disaster mitigation strategies and enhance regional preparedness for extreme weather events, particularly strong winds, which pose significant risks in Aceh Besar Regency, Indonesia.

MATERIALS AND METHODS

In this study, extreme weather hazards, specifically strong winds, were analyzed using a scoring method based on three key parameters: land openness, slope gradient, and annual rainfall. The scoring framework follows the guidelines outlined in BNPB Regulation No. 2 of 2012. The hazard mapping process relies on spatial data, as presented in Table 1, to systematically assess and classify areas at risk of extreme weather events. Aceh Besar Regency was selected as the study area (Figure 2).

All analytical processes were conducted using GIS, as seen in Figure 1. Before initiating the analysis, it is essential to standardize the coordinate system for all datasets by reprojecting them to the Universal Transverse Mercator (UTM) or World Mercator coordinate system. This standardization ensures that mathematical analyses can be performed directly using a uniform unit of measurement in meters, thereby improving the accuracy and consistency of spatial calculations.

Slope analysis, DEM data was analyzed to generate slope information, which serves as a key parameter influencing the potential impact of strong winds in a given area. Regions with gentle slopes are more susceptible to strong winds compared to steeper terrains.

Land cover classification, land cover data was analyzed to classify different types of land cover relevant to extreme weather conditions. The classification was divided into three categories, each assigned specific scores and weights, as shown in Table 2.

Rainfall data mapping, annual rainfall data was obtained from the most recent datasets provided by authorized institutions such as the Meteorology, Climatology, and Geophysics Agency (BMKG). If unavailable, alternative data sources, such as CHIRPS (Climate Hazards Group Infra-Red Precipitation), were used. In this study, annual rainfall data from CHIRPS for the period 1988–2017 in Aceh Besar Regency was utilized. The next step involved normalizing rainfall values

Table 1. Spatial data for extreme weather hazards

Type	Form	Source
Administrative boundaries	GIS vektor (Polygon)	BIG/Bappeda
Land cover	GIS vektor (Polygon)	BIG/KLHK/Bappeda
Annual rainfall map	GIS vektor (Polygon)	BMKG/ CHIRPS 2 USGS
DEM (Digital Elevation Model)	GIS raster (Grid)	LAPAN/NASA/JAXA

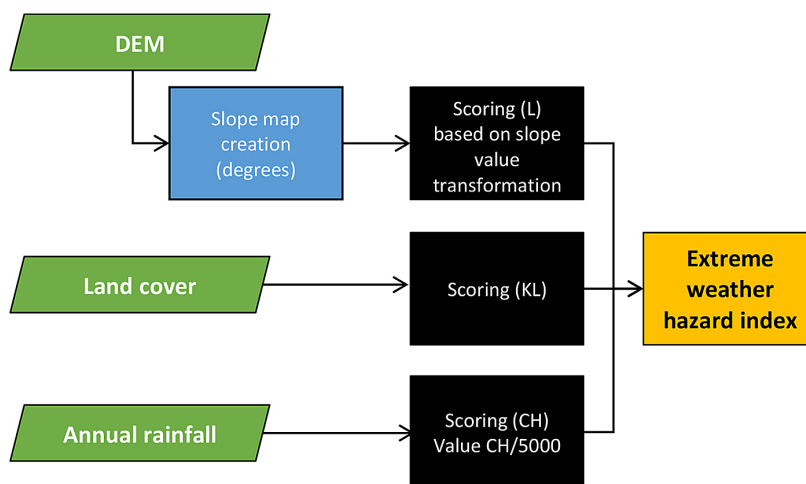


Figure 1. Process flow for creating extreme weather hazard index

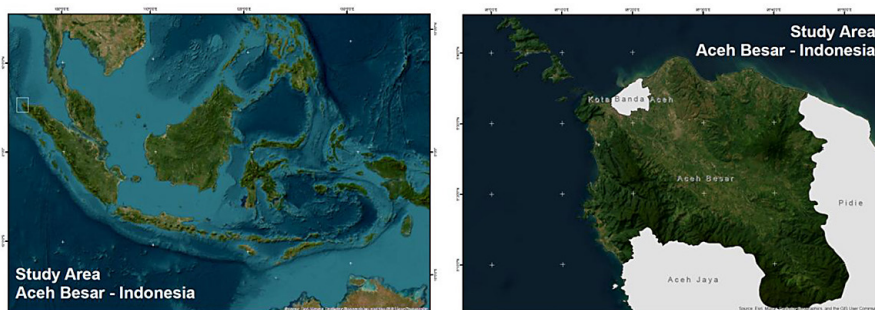


Figure 2. Study area

Table 2. Land cover classification parameters

Land cover type	Score
Forest	0.333
Plantation/Agricultural land	0.666
Shrubland, grassland, dry fields	1

by dividing the recorded precipitation by 5000 mm, which represents the approximate maximum annual rainfall in Indonesia.

Hazard index calculation, as previously mentioned, the Extreme Weather Hazard Index was determined through an overlay of the three key parameters: slope, land cover, and annual rainfall. The hazard classification follows BNPB Regulation No. 2/2012, with the following thresholds are low hazard as ≤ 1 , moderate hazard as $1 \leq 3$, high hazard as > 3 .

Slope class generalization, the hazard index calculation may produce sporadic hazard pixels, which require generalization to enhance spatial consistency. To address this, slope class generalization was performed using DEM data, ensuring a more cohesive and interpretable hazard map.

RESULTS AND DISCUSSION

The extreme weather hazard analysis was conducted through the processing of digital elevation model (DEM) data to generate a slope map, which serves as a key parameter in assessing the potential impact of strong winds. Additionally, land cover classification was performed based on BNPB Regulation No. 2, allowing for the evaluation of regional vulnerability levels. Furthermore, annual rainfall mapping was carried out using CHIRPS data from 1988 to 2017, normalized against the maximum recorded rainfall in Indonesia. The overlay of these three parameters are slope, land cover, and rainfall, produced an extreme weather hazard index categorized into three risk levels: low, moderate, and high. To refine the results and eliminate the presence of sporadic hazard pixels, a slope class generalization process was applied. The final hazard distribution can be observed in Figure 3.

Figure 4, general distribution of low area (km²) of extreme weather hazard are the average low area per village is 0.198 km², but the data shows

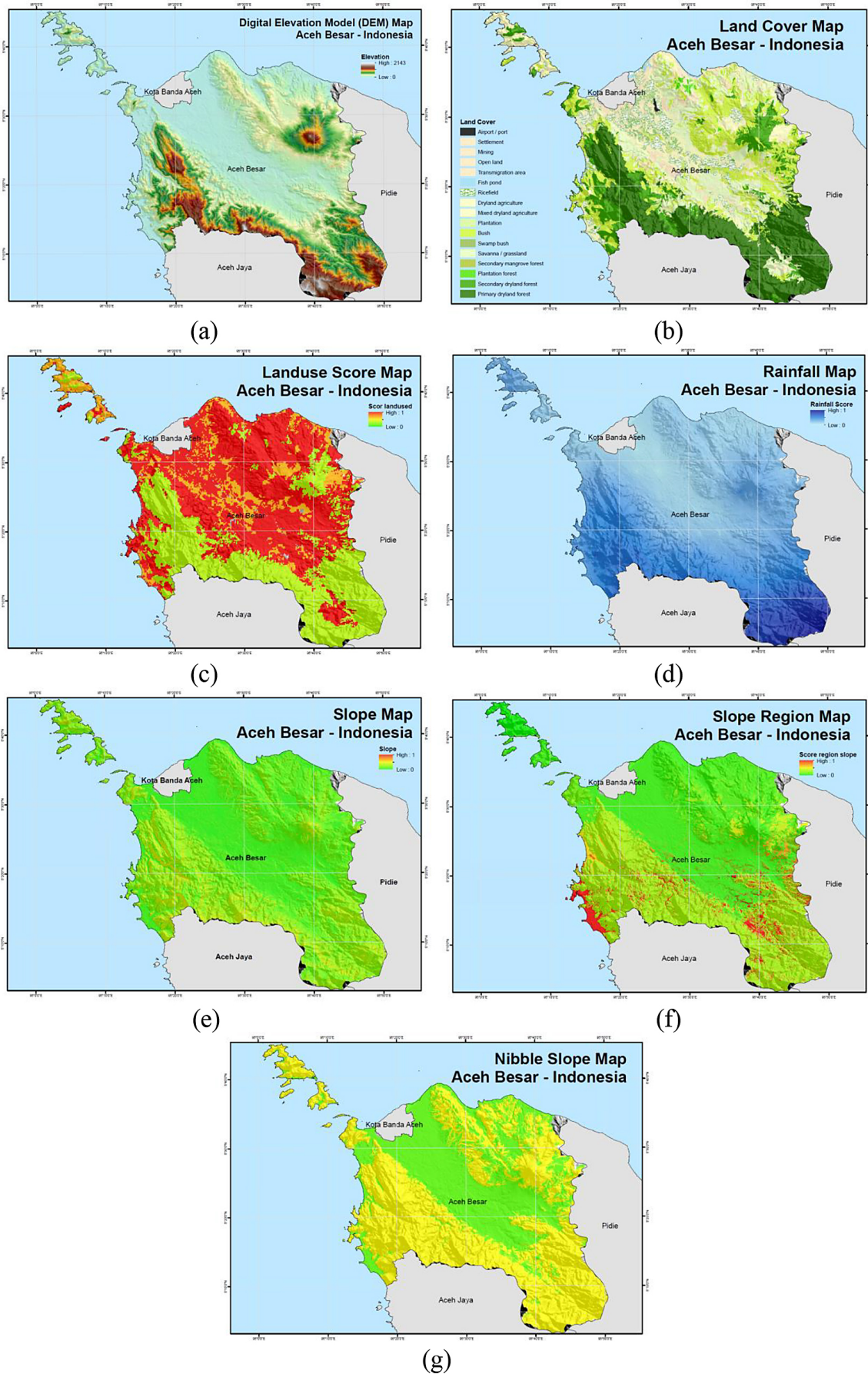


Figure 3. (a) Digital elevation model, (b) land cover map, (c) landuse score map, (d) rainfall map, (e) slope map, (f) slope region map, and (g) nibble slope map

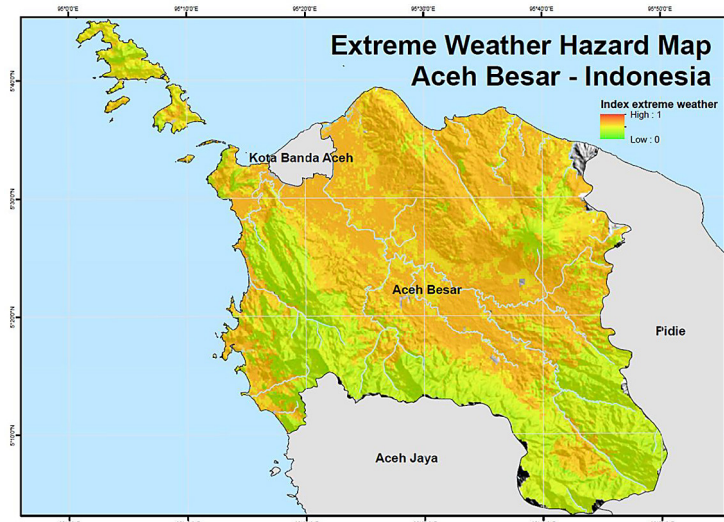


Figure 4. Extreme weather hazard map for Aceh Besar

high variation, as indicated by a standard deviation of 1.057 km². The minimum value is 0 km², meaning some villages have no low-lying areas, while the maximum value is 11.44 km². Prevalence of zero low area of extreme weather hazard is out of 604 villages, 533 villages (88.2%) have 0 km² of low area. This suggests that only a small percentage of villages actually contain significant low-lying land. Villages with the largest low areas of extreme weather hazard are Suka Tani (11.44 km²), Bak Sukon (10.18 km²), Bueng (9.02 km²), Meunasah Bak U (8.24 km²), Siron Krueng (7.95 km²). These villages have significantly larger low-lying areas compared to the majority of others. Possible implications are the high number of villages with zero or minimal low areas suggests that most areas in this dataset are located in elevated or non-flood-prone regions. The few villages with high low-area values might be more vulnerable to water accumulation and potential flooding, especially during heavy rainfall.

General distribution of moderate area of extreme weather hazard (km²) are the average moderate area per village is 3.90 km², but there is a high variation, as indicated by a standard deviation of 13.59 km² (Figure 4). The minimum value is 0 km², meaning some villages have no moderate area, while the maximum value is 197.59 km². Prevalence of zero moderate area are out of 604 villages, 46 villages (7.6%) have 0 km² of moderate area, which is significantly lower compared to the “low area” category. This suggests that most villages in this dataset contain at least some moderate-lying areas. Villages with the largest moderate areas are Bueng (197.59 km²), Suka Tani

(168.12 km²), Bak Sukon (112.66 km²), Meurah (74.36 km²), and Lamtamot (61.08 km²). These villages have significantly larger moderate areas of extreme weather hazard compared to the majority of others. Possible implications are the presence of larger moderate-lying areas suggests these villages might be situated in gently sloping or undulating terrains, which could influence land use patterns such as agriculture, settlement expansion, or conservation areas. Villages with higher moderate areas of extreme weather hazard may also play a role in water retention and drainage, impacting flood management strategies.

The analyzed data includes various villages in Lhoong sub-district, each exhibiting different levels of extreme weather hazard risk. Examining the relationship between village elevation and village names provides insights into the geographical characteristics and elevation distribution patterns in the region. Some villages have relatively low elevation values, while others show higher values. Specifically, Meunasah Krueng Kala and Jantang both have an elevation of 0.096952 km², Baroh Krueng Kala has 0.581713 km², Tunong Krueng Kala has 0.775618 km², and Sungko Mulat has 0.387809 km². The analysis reveals variations in elevation among villages in Lhoong sub-district. While some villages exhibit low elevation values, others are significantly higher.

The histogram represent in Figure 5a, the distribution of low area of extreme weather hazard (km²) across various villages. The data appears to be right-skewed, meaning that most villages have relatively small low areas, while only a few villages have significantly larger values

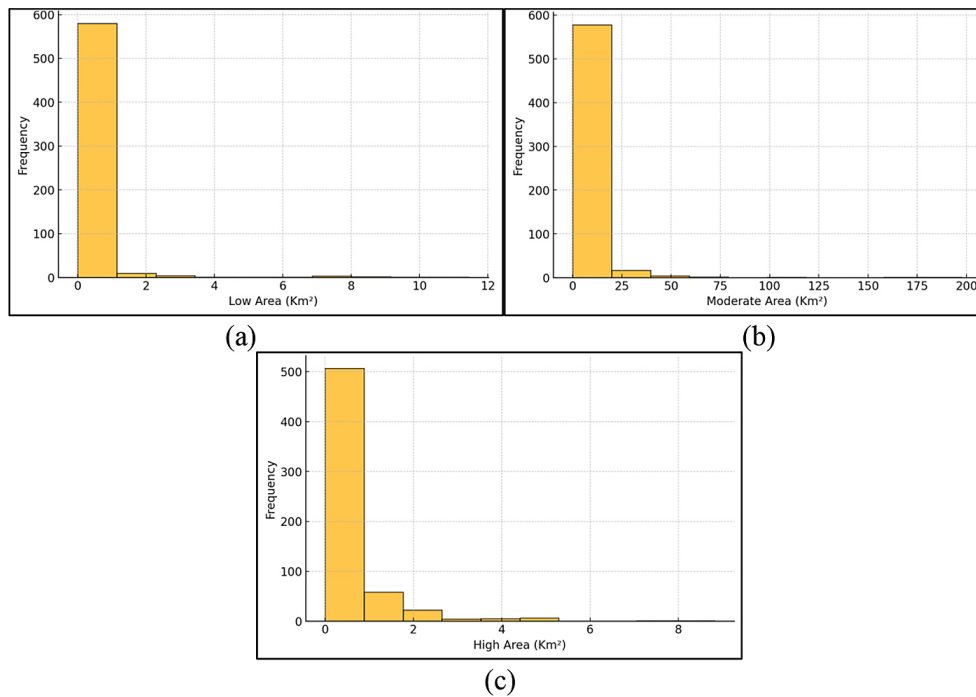


Figure 5. Histogram distribution of across villages: (a) low area (km²), (b) moderate area (km²), and high area (km²)

(Ammatawiyanon et al., 2022; Handiani et al., 2022). The presence of a long tail on the right suggests that there are some villages with larger low areas, which could be considered outliers. A majority of villages have low values of low area of extreme weather hazard (km²), clustering around the lower end of the distribution. The highest frequency occurs in the 0–0.5 km² range, indicating that most villages have small low-lying areas. The variation in low areas among villages could be influenced by geographical factors such as topography, river proximity, and land use (Dai et al., 2017; Gao et al., 2023). Some villages may be located in naturally lower regions, while others have minimal low-lying areas due to elevation differences.

The histogram reveals in Figure 5b, that the majority of villages have relatively small moderate area values, with a high concentration in the lower range of the distribution. The frequency decreases as the moderate area increases, indicating a right-skewed distribution. This suggests that while most villages have small to moderate areas of gently sloping terrain, a few villages possess significantly larger moderate area extents. The statistical parameters derived from the dataset support this observation are the mean moderate area per village is approximately 3.90 km², with a standard deviation of 13.59 km². A significant proportion of villages exhibit moderate areas

below 5 km², suggesting a dominance of small-sized moderate terrain regions. The maximum observed value is 197.59 km², which is substantially higher than the mean, indicating the presence of outliers. Approximately 7.6% of villages have zero moderate area, highlighting regions that lack transitional terrains.

Figure 5c illustrates that the majority of villages have relatively small high-elevation areas, with the highest frequency occurring within the 0–2 km² range. While some villages exhibit larger high-elevation areas, their frequency is significantly lower, indicating that villages with extensive high-elevation areas are less common. The peak frequency within the 0–2 km² range suggests that most villages in the study area have small high-elevation areas. Additionally, as high-elevation area size increases, the number of villages decreases, demonstrating an inverse relationship between elevation area size and village frequency. A few villages exhibit exceptionally large high-elevation areas, which are represented on the right tail of the histogram. These villages can be considered outliers, as their high-elevation areas are significantly larger compared to most other villages in the region.

Table 3, Most sub-districts exhibit a larger proportion of Moderate Area compared to Low and High Areas. For example, Kota Jantho (518 km²), Seulimeum (327 km²), and Lembah Seulawah

Table 3. The impact area of extreme weather hazard analysis (in km²)

Sub-district name	Low (km ²)	Moderate (km ²)	High (km ²)
Lhoknga	28	182	24
Indrapuri	3	172	27
Seulimeum	2	327	58
Montasik	0	44	19
Sukamakmur	0	34	10
Darul Imarah	0	11	13
Peukan Bada	2	25	6
Mesjid Raya	0	111	15
Ingin Jaya	0	10	14
Kuta Baro	0	47	13
Darussalam	0	28	11
Pulo Aceh	3	77	2
Lembah Seulawah	6	270	32
Kota Jantho	27	518	31
Kota Cot Glie	24	264	30
Kuta Malaka	0	19	4
Simpang Tiga	0	21	6
Darul Kamal	0	19	5
Baitussalam	0	10	9
Krueng Barona Jaya	0	3	3
Leupung	26	135	5
Blang Bintang	0	29	13

(270 km²) have the highest moderate land coverage. This suggests that these areas consist of land with moderate environmental or land-use characteristics, possibly including agricultural land, mixed-use forests, or transitional zones between urban and rural areas. The presence of Low Area is highly uneven across sub-districts. Some regions, such as Montasik, Sukamakmur, Darul Imarah, Ingin Jaya, and Darussalam, report no low area coverage, while Lhoknga (28 km²), Kota Jantho (27 km²), and Kota Cot Glie (24 km²) have relatively high low area coverage. This might indicate differences in land use planning, geographical conditions, or zoning regulations. The High Area distribution follows a different pattern, with the highest values observed in Seulimeum (58 km²), Lembah Seulawah (32 km²), and Indrapuri (27 km²). These sub-districts might contain rugged terrain, conservation zones, or areas designated for specific land uses such as protected forests or hilly landscapes. Some sub-districts exhibit unique distributions (Figure 6). For instance, Pulo Aceh has a significantly low High Area (2 km²) despite having a relatively moderate amount of Low and Moderate areas. Similarly, Leupung has a higher Low

Area (26 km²) but relatively small High Area (5 km²), possibly due to its coastal and hilly geography. More urbanized or coastal sub-districts, such as Baitussalam, Krueng Barona Jaya, and Peukan Bada, tend to have lower values for all categories, particularly in High Areas. This may indicate land limitations due to population density, infrastructure, or coastal landforms.

Several studies have analyzed extreme weather hazards using geospatial or GIS-based approaches across different regions. For instance, a study in Arkansas employed GIS-based regression analysis to assess the influence of topography, land cover, and other factors on hazard mitigation and building code improvements (Rowden and Aly, 2018). Similarly, another study predicted extreme wind speeds in Switzerland using GIS and generalized additive models, regionalizing wind statistics based on topographic and landscape variables (Etienne, et al., 2010). In Australia’s Great Barrier Reef, researchers analyzed cyclone-induced reef damage using a cyclone wind hindcasting model within GIS to reconstruct high-energy wind and wave conditions over time (Puotinen, 2007; Duvat et al., 2019). A separate

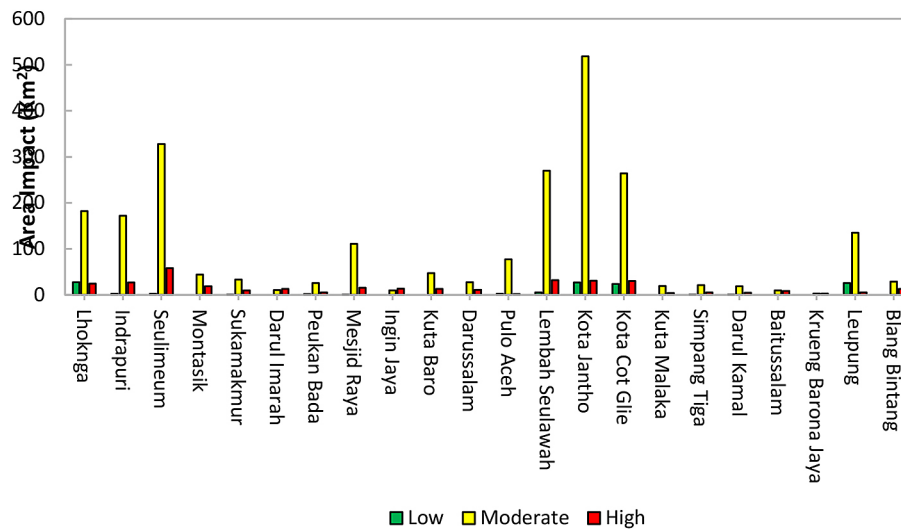


Figure 6. Sub-districts affected by extreme weather hazards

study developed an integrated monitoring and forecasting system for managing seaport safety under extreme wind events, which was tested using selected intense weather cases (Repetto et al., 2017; Athanasatos et al., 2014; Rawson et al., 2021). Furthermore, hurricane exposure modeling in Cusuco National Park, Honduras, integrated a wind pressure and exposure model with historical hurricane data to assess risk levels (Batke et al., 2014). Coastal vulnerability to tropical cyclones in Odisha, India, was also evaluated using a GIS-based approach, applying the coastal vulnerability index (CVI) to quantify risk levels (Sahoo and Bhaskaran, 2018). Additionally, hazardous weather events affecting river transport in Novi Sad, Serbia, were analyzed using GIS, geo-statistics, and numerical methods to assess port vulnerability and adaptation strategies (Komazec et al., 2024). These studies highlight the versatility of GIS-based approaches in analyzing extreme weather hazards, emphasizing their role in hazard prediction, vulnerability assessment, and risk mitigation across diverse geographic regions.

CONCLUSIONS

This study has analyzed the distribution of extreme weather hazards in Aceh Besar using a geospatial approach with GIS-based overlay techniques. The results indicate significant variations in low, moderate, and high hazard areas across different villages, highlighting the influence of topographical and environmental factors. The findings reveal that low-hazard areas are generally minimal

across most villages, with 88.2% of villages having no significant low-lying zones. However, a few villages, such as Suka Tani, Bak Sukon, and Bueng, exhibit substantial low-hazard areas, suggesting potential vulnerability to water accumulation and flooding. The distribution of moderate-hazard areas presents a different pattern, with an average of 3.90 km² per village but a high variation, indicating a mix of gently sloping terrains. Villages like Bueng, Suka Tani, and Bak Sukon contain the largest moderate-hazard areas, which may influence land use and flood management strategies. In contrast, high-hazard areas are less frequent, with a majority of villages exhibiting small high-terrain zones, suggesting that steep terrains are relatively rare. The histogram analysis further supports these findings, showing a right-skewed distribution for low and moderate hazard areas, meaning that most villages have small hazard zones, while only a few have large extents. This pattern suggests that extreme weather hazards are concentrated in specific locations rather than evenly distributed across the region. These results emphasize the importance of targeted disaster mitigation strategies. Villages with extensive low-hazard areas require enhanced flood risk management, while those with moderate-hazard zones should focus on land use planning and erosion control. Further studies should explore the relationship between hazard distribution and environmental factors such as river proximity, land cover changes, and climate trends. Integrating these insights into regional disaster preparedness plans can enhance community resilience and reduce the adverse impacts of extreme weather events in Aceh Besar.

Acknowledgements

The authors would like to thank Prof. Akhyar and Fikri kurniawan for her technical support throughout this research.

REFERENCES

- BNPB (2012). Peraturan Kepala Badan Nasional Penanggulangan Bencana Nomor 02 Tahun 2012 Tentang Pedoman Umum Pengkajian Risiko Bencana [Perka BNPB 2/2012: Regulation of the Head of the National Disaster Management Agency Number 02 of 2012 About General Guidelines for Disaster Risk Assessment]. Indonesian. Accessed 10 August 2022. <https://bnpb.go.id/uploa ds/migration/pubs/30.pdf>
- Wang, B., Ding, Y. & Sikka, D.R. (2006). Synoptic systems and weather. *The asian monsoon*, 131–201. https://doi.org/10.1007/3-540-37722-0_4
- Akande, A., Costa, A.C., Mateu, J. & Henriques, R. (2017). Geospatial analysis of extreme weather events in Nigeria (1985–2015) using self-organizing maps. *Advances in Meteorology*, 2017(1), 1–11. <https://doi.org/10.1155/2017/8576150>
- Sugianto, S., Rusdi, M., Budi, M. & Farhan, A., Akhyar, A. (2023). agricultural droughts monitoring of aceh besar regency rice production center, Aceh, Indonesia—application vegetation conditions index using Sentinel-2 image data. *Journal of Ecological Engineering*, 24(1), 159–171. <https://doi.org/10.12911/22998993/155999>
- Chen, Y. (2022). Flood hazard zone mapping incorporating geographic information system (GIS) and multi-criteria analysis (MCA) techniques. *Journal of Hydrology*, 612, 128268. <https://doi.org/10.1016/j.jhydrol.2022.128268>
- Kocsis, I., Bilaşco, Ş., Irimuş, I.A., Dohotar, V., Rusu, R. & Roşca, S. (2022). Flash flood vulnerability mapping based on FFPI using GIS spatial analysis case study: Valea Rea catchment area, Romania. *Sensors*, 22(9), 1–21. <https://doi.org/10.3390/s22093573>
- Diriba, D., Takele, T., Karuppanan, S. & Husein, M. (2024). Flood hazard analysis and risk assessment using remote sensing, GIS, and AHP techniques: a case study of the Gidabo Watershed, main Ethiopian Rift, Ethiopia. *Geomatics, Natural Hazards and Risk*, 15(1), 1–19. <https://doi.org/10.1080/19475705.2024.2361813>
- Gigović, L., Pamučar, D., Bajić, Z. & Drobnjak, S. (2017). Application of GIS-interval rough AHP methodology for flood hazard mapping in urban areas. *Water*, 9(6), 1–26. <https://doi.org/10.3390/w9060360>
- Chau, V.N., Holland, J., Cassells, S. & Tuohy, M. (2013). Using GIS to map impacts upon agriculture from extreme floods in Vietnam. *Applied Geography*, 41, 65–74. <https://doi.org/10.1016/j.apgeog.2013.03.014>
- Raghuvanshi, T.K., Negassa, L. & Kala, P.M. (2015). GIS based Grid overlay method versus modeling approach—A comparative study for landslide hazard zonation (LHZ) in Meta Robi District of West Showa Zone in Ethiopia. *The Egyptian Journal of Remote Sensing and Space Science*, 18(2), 235–250. <https://doi.org/10.1016/j.ejrs.2015.08.001>
- Basharat, M., Shah, H.R. & Hameed, N. (2016). Landslide susceptibility mapping using GIS and weighted overlay method: a case study from NW Himalayas, Pakistan. *Arabian Journal of Geosciences*, 9, 1–19. <https://doi.org/10.1007/s12517-016-2308-y>
- Metternicht, G., Humi, L. & Gogu, R. (2005). Remote sensing of landslides: An analysis of the potential contribution to geo-spatial systems for hazard assessment in mountainous environments. *Remote sensing of Environment*, 98(2–3), 284–303. <https://doi.org/10.1016/j.rse.2005.08.004>
- Aksha, S.K., Resler, L.M., Juran, L. & Carstensen Jr, L.W. (2020). A geospatial analysis of multi-hazard risk in Dharan, Nepal. *Geomatics, Natural Hazards and Risk*, 11(1), 88–111. <https://doi.org/10.1080/19475705.2019.1710580>
- Hoque, M.A.A., Pradhan, B. & Ahmed, N. (2020). Assessing drought vulnerability using geospatial techniques in northwestern part of Bangladesh. *Science of the Total Environment*, 705, 135957. <https://doi.org/10.1016/j.ocecoaman.2019.104898>
- Hoque, M.A.A., Phinn, S., Roelfsema, C. & Childs, I. (2018). Assessing tropical cyclone risks using geospatial techniques. *Applied geography*, 98, 22–33. <https://doi.org/10.1016/j.apgeog.2018.07.004>
- Chen, K., Blong, R. & Jacobson, C. (2003). Towards an integrated approach to natural hazards risk assessment using GIS: with reference to bushfires. *Environmental management*, 31, 0546–0560. <https://doi.org/10.1007/s00267-002-2747-y>
- Hashim, H.Q. & Sayl, K.N. (2021). Detection of suitable sites for rainwater harvesting planning in an arid region using geographic information system. *Applied Geomatics*, 13, 235–248. <https://doi.org/10.1007/s12518-020-00342-3>
- Walke, N., Reddy, G.O., Maji, A.K. & Thayalan, S. (2012). GIS-based multicriteria overlay analysis in soil-suitability evaluation for cotton (*Gossypium* spp.): A case study in the black soil region of Central India. *Computers & Geosciences*, 41, 108–118. <https://doi.org/10.1016/j.cageo.2011.08.020>
- Farhan, A., Nasution, A.I. & Akhyar (2024). Earthquake disaster map using GIS analysis: a case study of Bener Meriah-Aceh, Indonesia. *Arabian*

- Journal of Geosciences*, 17(53), 1–15. <https://doi.org/10.1007/s12517-023-11850-y>
20. Akhyar & Sary, C.A. (2024). Identification of geothermal potential zone associated with land surface temperature derived from Landsat 8 data using split-window algorithm. *Journal of Applied Research and Technology*, 22(1), 125–137. <https://doi.org/10.22201/icat.24486736e.2024.22.1.2091>
 21. Budi, M. & Akhyar, H. (2021). Green open space detection and mapping using planetscope-3A image with vegetation index approach and supervised classification in Banda Aceh, Indonesia. *In Forum Geografic*, 20(2), 145–159. <https://doi.org/10.5775/fg.2021.034.d>
 22. Ammatawiyanon, L., Tongkumchum, P., Lim, A. & McNeil, D. (2022). Modelling malaria in southernmost provinces of Thailand: a two-step process for analysis of highly right-skewed data with a large proportion of zeros. *Malaria Journal*, 21(1), 1–10. <https://doi.org/10.1186/s12936-022-04363-8>
 23. Handiani, D.N., Heriati, A. & Gunawan, W.A. (2022). Comparison of coastal vulnerability assessment for Subang regency in north coast West Java-Indonesia. *Geomatics, Natural Hazards and Risk*, 13(1), 1178–1206. <https://doi.org/10.1080/19475705.2022.2066573>
 24. Dai, X., Zhou, Y., Ma, W. & Zhou, L. (2017). Influence of spatial variation in land-use patterns and topography on water quality of the rivers inflowing to Fuxian Lake, a large deep lake in the plateau of southwestern China. *Ecological Engineering*, 99, 417–428. <https://doi.org/10.1016/j.ecoleng.2016.11.011>
 25. Gao, C., Wu, Y., Bian, C. & Gao, X. (2023). Spatial characteristics and influencing factors of Chinese traditional villages in eight provinces the Yellow River flows through. *River Research and Applications*, 39(7), 1255–1269. <https://doi.org/10.1002/rra.3880>
 26. Rowden, K.W. & Aly, M.H. (2018). GIS-based regression modeling of the extreme weather patterns in Arkansas, USA. *Geoenvironmental Disasters*, 5, 1–15. <https://doi.org/10.1186/s40677-018-0098-0>
 27. Etienne, C., Lehmann, A., Goyette, S., Lopez-Moreno, J.I. & Beniston, M. (2010). Spatial predictions of extreme wind speeds over Switzerland using generalized additive models. *Journal of applied meteorology and climatology*, 49(9), 1956–1970. <https://doi.org/10.1175/2010JAMC2206.1>
 28. Puotinen, M.L. (2007). Modelling the risk of cyclone wave damage to coral reefs using GIS: a case study of the Great Barrier Reef, 1969–2003. *International Journal of Geographical Information Science*, 21(1), 97–120. <https://doi.org/10.1080/13658810600852230>
 29. Duvat, V., Pillet, V., Volto, N., Krien, Y., Cécé, R. & Bernard, D. (2019). High human influence on beach response to tropical cyclones in small islands: Saint-Martin Island, Lesser Antilles. *Geomorphology*, 325, 70–91. <https://doi.org/10.1016/j.geomorph.2018.09.029>
 30. Repetto, M.P., Burlando, M., Solari, G., De Gaetano, P. & Pizzo, M. (2017). Integrated tools for improving the resilience of seaports under extreme wind events. *Sustainable cities and society*, 32, 277–294. <https://doi.org/10.1016/j.scs.2017.03.022>
 31. Athanasatos, S., Michaelides, S. & Papadakis, M. (2014). Identification of weather trends for use as a component of risk management for port operations. *Natural hazards*, 72(1), 41–61. <https://doi.org/10.1016/j.jweia.2012.03.029>
 32. Rawson, A., Brito, M., Sabeur, Z. & Tran-Thanh, L. (2021). A machine learning approach for monitoring ship safety in extreme weather events. *Safety science*, 141, 105336. <https://doi.org/10.1016/j.ssci.2021.105336>
 33. Batke, S.P., Jocque, M. & Kelly, D.L. (2014). Modelling hurricane exposure and wind speed on a mesoclimate scale: a case study from Cusuco NP, Honduras. *PloS one*, 9(3), p.e91306. <https://doi.org/10.1371/journal.pone.0091306>
 34. Sahoo, B. & Bhaskaran, P.K. (2018). Multi-hazard risk assessment of coastal vulnerability from tropical cyclones—A GIS based approach for the Odisha coast. *Journal of environmental management*, 206, 1166–1178. <https://doi.org/10.1016/j.jenvman.2017.10.075>
 35. Komazec, N., Šoškić, S., Milić, A., Štrbac, K. & Valjarević, A. (2024). Water transportation planning in connection with extreme weather conditions; case study—Port of Novi Sad, Serbia. *Open Geosciences*, 16(1), 1–13. <https://doi.org/10.1515/geo-2022-0559>